Available online at www.sciencedirect.com
ScienceDirect
Scripta Materialia 56 (2007) 33–36
Scripta MATERIALIA
www.actamat-journals.com

The formation of ordered structures in InGaN layers

M. Rao,* N. Newman and S. Mahajan

School of Materials, College of Liberal Arts and Sciences and Ira A. Fulton School of Engineering, Arizona State University, Tempe, AZ 85287-8706, USA

Received 13 June 2006; revised 28 August 2006; accepted 29 August 2006
Available online 6 October 2006

We investigated atomic ordering in $In_xGa_{1-x}N$ layers for x between 0.03 and 0.28 using transmission electron microscopy. We demonstrate that $\{10-11\}$ facets play a role in 1:1 ordering. Deviations in composition from $x = 0.5$ are accommodated by the formation of small ordered regions embedded in a short-range ordered or disordered matrix.

Keywords: Chemical vapor deposition (CVD); Transmission electron microscopy (TEM); Group III nitrides; Compound semiconductors; Ordering

A consensus has emerged that atomic species that are arranged in mixed III–V epitaxial layers, and have different covalent tetrahedral radii, are not distributed at random on their respective sublattices in the zinc-blende structure [1]. Two types of deviations from randomness are observed: phase separation and atomic ordering. Phase separation occurs on the surface while the layer is growing and reduces the strain energy of the system. Atomic ordering is caused by surface reconstruction-induced subsurface stresses that bias the occupation of certain sites according to the tetrahedral radii of the various atomic species.

Recent observations of atomic ordering in InGaN layers grown by metalorganic chemical vapor deposition (MOCVD) [2] and molecular beam epitaxy (MBE) [3] and phase separation in MOCVD-grown layers [4,5] are consistent with the above assessment. This is because the difference between the tetrahedral radii of In and Ga atoms is substantial. Behbehani et al. [2] observed ordered structures that had different periods along the [0001] direction. On the other hand, the observations of Doppalapudi et al. [3] are consistent with the doubling of real space periodicity along the [0001] direction, i.e., 1:1 order. In addition, they observed that the intensity of 1:1 ordering increases with increasing growth rate. This is counterintuitive.

Northrup et al. [6] performed first-principle calculations to understand the role of $\{10-11\}$ facets in 1:1 ordering. They found that surface reconstruction could occur on these facets, giving rise to alternating sites with N-coordination of 1 and 2. They showed that during the growth of InGaN on these facets, it is energetically more favorable for In atoms, rather than Ga atoms, to occupy sites of lower N-coordination. If it is assumed that In and Ga attach preferentially to these sites and that the layer grows by the migration of $\{10-11\}$ facets, a 1:1 ordered structure could evolve.

Three interesting questions arise from the preceding discussion. First, are $\{10-11\}$ facets involved in 1:1 atomic ordering in InGaN layers? Second, since In contents in most of the studies are not close to $x = 0.5$, how is deviation from the $In_{0.5}Ga_{0.5}N$ composition accommodated microstructurally in ordered layers? Third, how does growth rate influence ordering. We address these three issues in the present paper.

Previously, Lorenz et al. [7] and Narayanan et al. [8] showed that low-temperature (LT) GaN nucleation layers (NLs), grown on (0001) sapphire substrates, undergo metamorphosis on annealing at high temperature. The roughness increases on annealing, resulting in well-developed islands bounded by $\{10-11\}$ facets. Liliental-Weber et al. [9] demonstrated that V-defects observed in InGaN layers are associated with $\{10-11\}$ facets. These facets form on threading dislocations intersecting a free surface. The V-defects persist during growth and are not eliminated. Therefore, we used annealing of NLs and InGaN growth on thick GaN layers to produce $\{10-11\}$ facets in our study.

All growths were performed on epi-ready (0001) sapphire substrates in an Aixtron AIX200-RF MOCVD

* Corresponding author. Tel.: +1 480 965 4441; fax: +1 480 965 0037; e-mail: manu.rao@asu.edu

1359-6462/$ - see front matter
doi:10.1016/j.scriptamat.2006.08.068

horizontal reactor. The precursors were trimethylgallium (TMGa) trimethylindium and ammonia, and the reactor pressure was 300 mbar. Prior to the growth of GaN NLs, substrates were exposed to hydrogen at 1190 °C to desorb surface contaminants. The temperature was then lowered to 560 °C and 20 nm thick GaN NLs were deposited using hydrogen as a carrier gas. These NLs were subsequently annealed in ammonia and hydrogen to produce faceted GaN islands. Since the incorporation of indium into the growing InGaN film is relatively insensitive to precursor flow rates but is very sensitive to growth temperature [4], temperature was used to control the amount of indium incorporated. Set I samples were produced by depositing InGaN layers on faceted GaN islands using nitrogen as a carrier gas. For set II samples, 1.7 μm thick planar GaN layers were grown on annealed NLs at 1170 °C prior to the InGaN growth. InGaN layers were then deposited for 1 h. In addition, separate set II growths were performed with increased TMGa flowrates, resulting in an enhanced growth rate.

The thicknesses of the layers, as discerned by cross-sectional transmission electron microscopy (TEM), were approximately 400 nm at the standard growth rate and 900 nm at the higher growth rate. The compositions determined by Rutherford backscattering spectrometry (RBS) and InGaN growth temperatures were $In_{0.03}Ga_{0.97}N$ (928 °C), $In_{0.12}Ga_{0.88}N$ (910 °C), $In_{0.22}Ga_{0.78}N$ (880 °C) and $In_{0.28}Ga_{0.72}N$ (850 °C) at the standard growth rate. At the higher growth rate, $In_{0.14}Ga_{0.86}N$ (910 °C) and $In_{0.25}Ga_{0.75}N$ (825 °C) were grown. The as-grown InGaN layers were evaluated using $(10\bar{1}0)$ and $(11\bar{2}0)$ cross sections by TEM. TEM samples were prepared using dimpling, followed by cold stage ion-milling. The dimpling and ion-milling parameters were kept constant, in order to ensure that the samples have similar thickness. Diffraction patterns were collected using the same exposure time and selected area diffraction (SAD) aperture to ensure comparability of results.

Figure 1(a) shows a $(10\bar{1}0)$ SAD pattern taken from a set I $In_{0.28}Ga_{0.72}N$ layer. The $(10\bar{1}0)$ orientation was chosen because in this orientation the (0001) spot can only exist as a superlattice reflection. In the more commonly chosen $(11\bar{2}0)$ orientation, double diffraction can occur between the $(1\bar{1}01)$ and $(\bar{1}100)$ spots, leading to intensity at (0001). It is clear from Figure 1(a) that intensity maxima are present at the (0001) and $\{1/2, -1, 1/2, 1\}$ positions. The intensity at (0001) and other equivalent positions exists as sharp spots. The peak intensity of the (0001) spot is 1.14, relative to background. This is consistent with the occurrence of (1:1) ordering, as observed previously [2,3]. Similar features were seen in patterns taken from other set I samples.

Lines of diffuse intensity are also present in Figure 1(a) and these are oriented along the $\langle 1\bar{2}12 \rangle$ directions. These lines intersect at the $\{1/2, -1, 1/2, 1\}$ positions, resulting in intensity maxima. Cooling the specimen to liquid nitrogen temperature does not produce a significant change in the intensity of these lines, as shown in Figure 1(b), suggesting they are not caused by thermal diffuse scattering. The relative intensity of

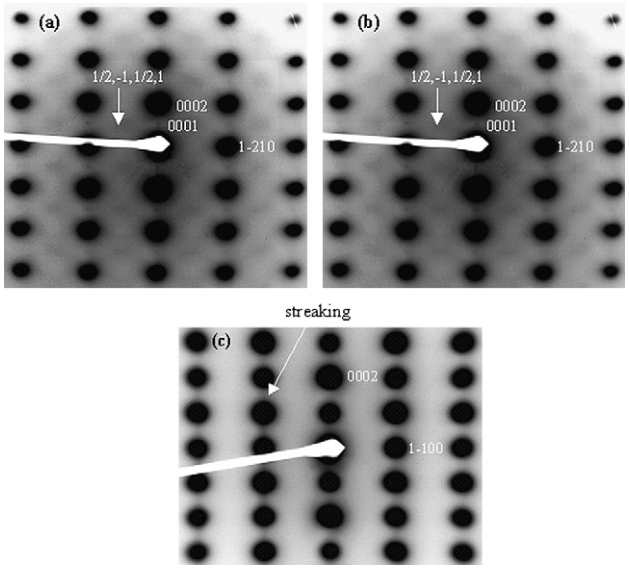

Figure 1. (a) A $(10\bar{1}0)$ SAD pattern taken from a set I $In_{0.28}Ga_{0.72}N$ layer at ambient temperature. Superlattice spots are present at (0001) and lines of diffuse intensity are oriented along the $\langle 1\bar{2}12 \rangle$ directions. (b) At liquid nitrogen temperature the diffuse intensity still exists, suggesting its origin is not thermal. (c) A $(11\bar{2}0)$ SAD pattern at ambient temperature. No diffuse intensity is present but streaking exists along the $[0001]$ direction. The patterns are displayed as negatives for clarity.

the (0001) spot is similar to that in Figure 1(a). Figure 1(c) shows a $(11\bar{2}0)$ SAD pattern taken from the same layer. In contrast to the $(10\bar{1}0)$ orientation, a network of diffuse intensity is not observed in this orientation. However, streaking is seen along the $[0001]$ direction through the diffraction spots, whereas no such streaking is present in the $(10\bar{1}0)$ orientation.

It is apparent that the Bragg spots in Figure 1 are noncircular. This is due to the presence of satellite spots, which are oriented along $\langle 11\bar{2}0 \rangle$ and $\langle 10\bar{1}0 \rangle$ directions, closely surrounding the fundamental reflections. Satellites form due to a diffraction effect associated with composition modulations lying within the growth plane [4,5].

Dark-field images were produced using the (0001) and $(1/2, -1, 1/2, 1)$ spots and the results are shown in Figure 2(a) and (b). In both these images, there appears to be a collection of bright regions, with diameters of approximately 10–20 nm, randomly embedded within a darker matrix. There does not appear to be a significant difference between the images formed using (0001) and $(1/2, -1, 1/2, 1)$ spots, suggesting that both short- and long-range order are present in the same regions.

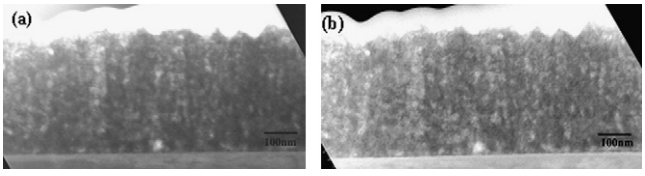

Figure 2. (a) Dark-field image from set I $In_{0.28}Ga_{0.72}N$ formed using the (0001) superlattice spot and (b) using the intensity maxima at $(1/2, -1, 1/2, 1)$.